Dynamic response of laminated and sandwich composite structures via 1D models based on Chebyshev polynomials

Dynamic response of laminated and sandwich composite structures via 1D models based on Chebyshev polynomials

A. Pagani*, M. Petrolo†, E. Carrera‡
MUL^2 Group, Department of Mechanical and Aerospace Engineering, Politecnico di Torino,
Corso Duca degli Abruzzi 24, 10129 Torino, Italy

Author for correspondence:
E. Carrera, Professor of Aerospace Structures and Aeroelasticity,
Department of Mechanical and Aerospace Engineering,
Politecnico di Torino,
Corso Duca degli Abruzzi 24,
10129 Torino, Italy,
tel: +39 011 090 6836,
fax: +39 011 090 6899,
e-mail: erasmo.carrera@polito.it

*Assistant Professor, e-mail: alfonso.pagani@polito.it
†Assistant Professor, e-mail: marco.petrolo@polito.it
‡Professor of Aerospace Structures and Aeroelasticity, e-mail: erasmo.carrera@polito.it

Abstract

This paper presents the dynamic response of composite structures via refined beam models. The mode superposition method was used, and the Carrera Unified Formulation (CUF) was exploited to create the advanced structural models. The finite element method was employed to compute the natural frequencies and modes. The main novelty of this paper concerns the use of Chebyshev polynomials to define the displacement field above the cross-section of the beam. In particular, polynomials of the second kind were adopted, and the results were compared with those from analytical solutions and already established CUF-based beam models, which utilize Taylor and Lagrange polynomials to develop refined kinematics theories. Sandwich beams and laminated, thin walled box beams were considered. Non-classical effects, such has the cross-section distortion and bending/torsion coupling were evaluated. The results confirm the validity of the CUF for the implementation of refined structural models with any expansion functions and orders. In particular, the Chebyshev polynomials provide accuracies very similar to those from Taylor models. The use of high order expansions, e.g. seventh order, leads to results as accurate as those of Lagrange models which, from previous publications, are known as the most accurate CUF 1D models for this type of structural problems.

Keywords: Refined beam theories, Finite elements, Carrera Unified Formulation, Dynamic response, Mode superposition.

1 Introduction

The development of one-dimensional (1D) structural models is of great interest to reduce the computational costs in many engineering applications. Advanced 1D models are required to have results as accurate as those of plate/shell (2D) and solid (3D) models. The Euler-Bernoulli Beam Theory (EBBT) [1] and the Timoshenko Beam Theory (TBT) [2, 3] are the classical beam theories. The TBT enhances EBBT assuming constant shear strains across the cross-section. Slender and moderately thick, solid-section beams subjected to bending can be analyzed with good accuracy using these theories. In the last decades, many refined beams theories have been proposed to improve classical models, but preserving their computational efficiency. Some of the most important are discussed here, with particular attention paid to structural dynamics and composite structures. More comprehensive reviews can be found in [4, 5].

The adoption of shear correction factors [6, 7] is a common way to improve classical theories, although correction factors are strongly problem dependent. Another approach exploits refined displacement field above the cross-section of the beam to include non-classical effects such as warping and cross-section distortions. Typical examples are those in [8–19].

This paper exploits refined beam models developed in the framework of the Carrera Unified Formulation (CUF). The CUF was initially developed for plates and shells [20, 21], and then extended to beams [22, 23]. In the CUF framework, refined structural models are built using expansions of the unknown variables. The number of terms of the expansion, i.e. the number of unknowns, can be chosen via a convergence analysis. The CUF has the great advantage to enable the implementation of any order structural models with no need of formal changes in the problem equations and matrices. Recently, the CUF 1D models have been used for structural dynamics; in particular, free-vibration [24–27] and dynamic response of thin walled structures [28]. In the works above, higher order beam theories were obtained using Taylor-like Expansion (TE). Lagrange expansions (LE) and the component-wise approach were used in [29–33]. In [34], trigonometric, exponential, and zig-zag models were used, whereas a beam theory based on Chebyshev Expansion (CE) polynomials has been introduced in [35]. CE models were then used for the dynamic response of typical aerospace structures in [36].

In the present work, the mode superposition method is combined with 1D CUF CE models to investigate the dynamic response of laminated structures. First, a simply supported beam subjected to a sinusoidal load is considered. Then, a sandwich structure subjected to harmonic loads and a composite box beam subjected to distributed loads are investigated. In this paper, Section 2 presents an overview of the higher order beam theories developed in the framework of CUF. Moreover, the FEM approach and mode superposition method are briefly outlined. Section 3 is devoted to the presentation of the results obtained using the proposed CUF, whereas conclusions are drawn in Section 4.

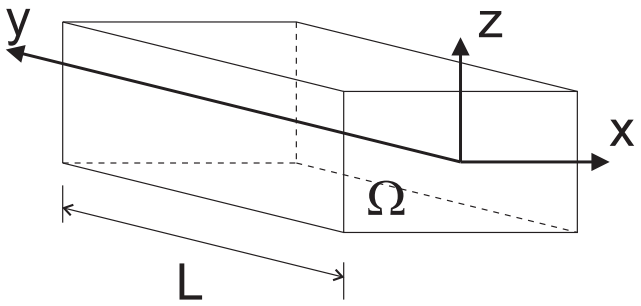

Figure 1: Coordinate frame of the beam.

2 Higher order, hierarchical models by CUF

Given a generic beam structure, the Cartesian coordinate system adopted is shown in Fig. 1. The cross-section Ω and the beam axis y, are orthogonal. Moreover, the beam axis has boundaries $0 \leq y \leq L$. The validity of the formulation adopted is not affected by the shape of the cross-section, since the reported rectangular cross-section has merely explicative purposes. The displacement field of a beam model in the framework of CUF can be written in a compact form as follows:

$$\mathbf{u}(x, y, z, t) = F_\tau(x, z)\mathbf{u}_\tau(y, t), \qquad \tau = 1, 2, ..., M \tag{1}$$

where $\mathbf{u} = \{u_x, u_y, u_z\}^T$ is the displacement vector; F_τ indicates the functions of the cross-section coordinates x and z; $\mathbf{u}_\tau$ is the generalized displacement vector; M indicates the number of terms in the expansion. The choice of F_τ and M is arbitrary. Thus, the basis functions adopted to model the displacement field across the section can be different and expanded to any order.

Considering Taylor-like expansion polynomials as F_τ functions, one can obtain the models referred to as TE. For instance, the displacement field of a second order TE model (TE2) can be expressed as follows:

$$\begin{aligned}
u_x(x, y, z, t) &= u_{x1}(y, t) + x\ u_{x2}(y, t) + z\ u_{x3}(y, t) + x^2\ u_{x4}(y, t) + xz\ u_{x5}(y, t) + z^2\ u_{x6}(y, t) \\
u_y(x, y, z, t) &= u_{y1}(y, t) + x\ u_{y2}(y, t) + z\ u_{y3}(y, t) + x^2\ u_{y4}(y, t) + xz\ u_{y5}(y, t) + z^2\ u_{y6}(y, t) \\
u_z(x, y, z, t) &= u_{z1}(y, t) + x\ u_{z2}(y, t) + z\ u_{z3}(y, t) + x^2\ u_{z4}(y, t) + xz\ u_{z5}(y, t) + z^2\ u_{z6}(y, t)
\end{aligned} \tag{2}$$

where u_{x_1}, u_{y_1}, u_{z_1}, ..., u_{z_6} represent the components of the generalized displacement vector, i.e. the unknown variables. The classical models - EBBT and TBT - can be obtained as particular cases of the TE1.

Another class of CUF models is based on Lagrange Expansions (LE). In this work, mainly bi-quadratic nine-node (L9) Lagrange polynomials are used as F_τ. Lagrange polynomials can be found in [23]. The displacement

field within an L9 element can be written as:

$$\begin{aligned} u_x(x,y,z) &= F_1(x,z)u_{x1}(y) + F_2(x,z)u_{x2}(y) + ... + F_9(x,z)u_{x9}(y) \\ u_y(x,y,z) &= F_1(x,z)u_{y1}(y) + F_2(x,z)u_{y2}(y) + ... + F_9(x,z)u_{y9}(y) \\ u_z(x,y,z) &= F_1(x,z)u_{z1}(y) + F_2(x,z)u_{z2}(y) + ... + F_9(x,z)u_{z9}(y) \end{aligned} \tag{3}$$

The time variable t is omitted in the following for the sake of clarity. $u_{x1}, ..., u_{z9}$ are the translational components of the nine points of the L9 element. L-elements can be assembled above the cross-section imposing the displacement continuity at the interface nodes.

In this paper, The Chebyshev Expansion (CE) is used for the first time to investigate the dynamic response of composite structures. For instance, the CE second order kinematic model (CE2) has 18 generalized displacement variables, and can be defined as follows:

$$\begin{aligned} u_x(x,y,z) &= P_{00}(x,z)u_{x1}(y) + P_{10}(x,z)u_{x2}(y) + P_{01}(x,z)u_{x3}(y) + P_{20}(x,z)u_{x4}(y) + P_{11}(x,z)u_{x5}(y) + P_{02}(x,z)u_{x6}(y) \\ u_y(x,y,z) &= P_{00}(x,z)u_{y1}(y) + P_{10}(x,z)u_{y2}(y) + P_{01}(x,z)u_{y3}(y) + P_{20}(x,z)u_{y4}(y) + P_{11}(x,z)u_{y5}(y) + P_{02}(x,z)u_{y6}(y) \\ u_z(x,y,z) &= P_{00}(x,z)u_{z1}(y) + P_{10}(x,z)u_{z2}(y) + P_{01}(x,z)u_{z3}(y) + P_{20}(x,z)u_{z4}(y) + P_{11}(x,z)u_{z5}(y) + P_{02}(x,z)u_{z6}(y) \end{aligned} \tag{4}$$

where P_{00}, ..., P_{02} are the Chebyshev polynomials of the second kind, as shown in [35].

2.1 Finite element formulation

The stress σ and the strain ϵ vectors are defined as follows:

$$\begin{aligned} \boldsymbol{\sigma} &= \{\sigma_{yy}, \sigma_{xx}, \sigma_{zz}, \sigma_{xz}, \sigma_{yz}, \sigma_{xy}\}^T \\ \boldsymbol{\epsilon} &= \{\epsilon_{yy}, \epsilon_{xx}, \epsilon_{zz}\epsilon_{xz}, \epsilon_{yz}, \epsilon_{xy}\}^T \end{aligned} \tag{5}$$

Under the assumption of small displacements and elongations, the following relation between strains and displacements holds:

$$\boldsymbol{\epsilon} = \boldsymbol{D}\boldsymbol{u} \tag{6}$$

$\boldsymbol{D}$ is the linear differential operator, defined as follows:

$$\boldsymbol{D} = \begin{bmatrix} 0 & \frac{\partial}{\partial y} & 0 \\ \frac{\partial}{\partial x} & 0 & 0 \\ 0 & 0 & \frac{\partial}{\partial z} \\ \frac{\partial}{\partial z} & 0 & \frac{\partial}{\partial x} \\ 0 & \frac{\partial}{\partial z} & \frac{\partial}{\partial y} \\ \frac{\partial}{\partial y} & \frac{\partial}{\partial x} & 0 \end{bmatrix} \tag{7}$$

Applying the constitutive law, one can obtain the stress components:

$$\boldsymbol{\sigma} = \tilde{\boldsymbol{C}}\boldsymbol{\epsilon} \tag{8}$$

For the sake of brevity, the explicit form of the coefficients $\tilde{\boldsymbol{C}}_{ij}$ in the previous relation is omitted. More details can be found in [37].

The shape functions N_i are used to interpolate the generalised displacement vector $\mathbf{u}_\tau$ along the y direction,

$$\boldsymbol{u}(x, y, z) = F_\tau(x, z)N_i(y)\boldsymbol{u}_{\tau i} \tag{9}$$

where $\mathbf{u}_{\tau i}$ is the nodal unknown vector. In the present work, four-node (B4) 1D elements have been used; this leads to a cubic approximation along the y axis. The internal strain energy L_{int} can be related to the work of the inertial loads L_{ine} according to the principle of virtual displacements:

$$\delta L_{int} = \int_V \delta\boldsymbol{\epsilon}^T \boldsymbol{\sigma}\, dV = -\delta L_{ine} \tag{10}$$

Where δ stands for virtual variation. The virtual variation of the strain energy can be written in a compact form combining Eqs. 6, 8 and 9:

$$\delta L_{int} = \delta\boldsymbol{u}_{sj}^T \mathbf{K}^{ij\tau s}\boldsymbol{u}_{\tau i} \tag{11}$$

In the above relation, the fundamental nucleus of the stiffness matrix is noted by $\mathbf{K}^{ij\tau s}$, whereas the four indexes indicated by the superscripts are those used to expand the elemental matrix. In particular, i and j are related to the shape functions N_i and N_j whereas τ and s are related to the expansion functions F_τ and F_s. The 3x3 array which represents the fundamental nucleus is formally independent of the order of the beam model. A more detailed explanation of the expansion of nuclei and assembly procedures in FEM framework can be found in [23]. The work of the inertial loadings can be written in terms of virtual variation,

$$\delta L_{ine} = \int_V \rho\delta\mathbf{u}^T\ddot{\mathbf{u}}\, dV \tag{12}$$

In the above equation ρ stands for the density of the material, whereas $\ddot{\mathbf{u}}$ is the acceleration vector. By substituting Eq. 9 into Eq. 12, one has

$$\delta L_{ine} = -\delta\boldsymbol{u}_{sj}^T \int_L N_i N_j\, dy \int_\Omega \rho F_\tau F_s\, d\Omega\ddot{\mathbf{u}}_{\tau i} = -\delta\boldsymbol{u}_{sj}^T \mathbf{M}^{ij\tau s}\ddot{\mathbf{u}}_{\tau i} \tag{13}$$

where $\mathbf{M}^{ij\tau s}$ is the fundamental nucleus of the elemental mass matrix and $\ddot{\mathbf{u}}_{\tau i}$ indicates the nodal acceleration vector. The components of the elemental mass are:

$$\mathbf{M}_{xx}^{ij\tau s} = \mathbf{M}_{yy}^{ij\tau s} = \mathbf{M}_{zz}^{ij\tau s} = \int_L N_i N_j \, dy \int_\Omega \rho F_\tau F_s \, d\Omega$$
$$\mathbf{M}_{xy}^{ij\tau s} = \mathbf{M}_{xz}^{ij\tau s} = \mathbf{M}_{yx}^{ij\tau s} = \mathbf{M}_{zx}^{ij\tau s} = \mathbf{M}_{yz}^{ij\tau s} = \mathbf{M}_{zy}^{ij\tau s} = 0 \tag{14}$$

It should be noted that no assumptions have been made on the expansion order of the theory, even in the case of the inertial terms. In fact, using this formulation, several refined beam models can be developed without any formal change in the fundamental nucleus components.

The fundamental nuclei are substituted into the principle of virtual displacement (Eq. 10)to obtain the undamped dynamic problem. The CUF fundamental nuclei are then expanded, and the global FEM arrays are assembled,

$$\mathbf{M}\ddot{\mathbf{u}} + \mathbf{K}\mathbf{u} = 0 \tag{15}$$

The second order system of ordinary differential equations is reduced into a classical eigenvalue problem if harmonic solutions are considered,

$$(-\omega_k^2 \mathbf{M} + \mathbf{K})\mathbf{u}_k = 0 \tag{16}$$

where $\mathbf{u}_k$ is the *k-th* eigenvector.

2.2 Mode superposition method

The equilibrium governing equations of the dynamic response in a system with multiple degrees of freedom (DOFs) are [38]:

$$\boldsymbol{M}\ddot{\boldsymbol{u}}(t) + \boldsymbol{C}\dot{\boldsymbol{u}}(t) + \boldsymbol{K}\boldsymbol{u}(t) = \boldsymbol{P}(t) \tag{17}$$

where $\boldsymbol{C}$ is the damping matrix, and $\boldsymbol{P}$ is the time-dependant loading vector, which is computed in the framework of CUF as in [23]. The unknowns vector $\boldsymbol{u}$ is transformed in accordance with the superposition method:

$$\boldsymbol{u}(t) = \boldsymbol{\Phi}\boldsymbol{x}(t) \tag{18}$$

where $\boldsymbol{\Phi}$ is a $DOFs \times m$ matrix containing m $\boldsymbol{M}$-orthonormalized eigenvectors and $\boldsymbol{x}(t)$ is a time-dependent vector of order m. To transform the equations of motion, each term of Eq. 18 is substituted into the governing equations (Eq. 17) and pre-multiplied by $\boldsymbol{\Phi}^T$

$$\ddot{\boldsymbol{x}}(t) + \boldsymbol{\Phi}^T\boldsymbol{C}\boldsymbol{\Phi}\dot{\boldsymbol{x}}(t) + \boldsymbol{\Omega}^2\boldsymbol{x}(t) = \boldsymbol{\Phi}^T\boldsymbol{P}(t) \tag{19}$$

where $\mathbf{\Omega}^2$ is the diagonal matrix that stores the eigenvalues ω_i^2. If the damping is neglected, from Eq. 19 one can notice that the equations of motion are decoupled. Hence, m individual equations can be obtained by decomposing this relation. The solution for each equation is computed by means of the Duhamel integral

$$\left.\begin{aligned} \ddot{x}_i(t) + \omega_i^2 x_i(t) &= r_i(t) \\ r_i(t) &= \mathbf{\Phi}_i \boldsymbol{P}(t) \end{aligned}\right\} \qquad i = 1, 2, ..., n \tag{20}$$

$$x_i(t) = \frac{1}{\omega_i} \int_0^t r_i(\tau) \sin \omega_i (t - \tau) d\tau + \alpha_i \sin \omega_i t + \beta_i \cos \omega_i t \tag{21}$$

To compute α_i and β_i, initial conditions need to be addressed. The contribution to the response for each mode is obtained after the solution for each of the m equations is calculated.

$$\boldsymbol{u}^m(t) = \sum_{i=1}^{m} \mathbf{\Phi}_i x_i(t) \tag{22}$$

In this approach, the accuracy of the solution depends on m.

3 Numerical Results

This section presents the numerical results of this paper. First, preliminary analyses were carried out on an isotropic structure. Then, a sandwich beam and a laminated box beam were considered.

3.1 Compact square section

A first, preliminary assessment is presented in this section to validate the modal superposition methodology. A simply supported, square section beam is considered. The cross-section height is 0.1 m, the span-to-height ratio L/h is 100, and the material properties are $E = 69$ GPa, $\nu = 0.33$ and $\rho = 2700\ \frac{kg}{m^3}$. A vertical, harmonic force was applied at the center of the mid-span section, $P_z(t) = P_{z0} sin(\omega t)$, where $P_{z0} = -1000N$ is the amplitude of the sinusoidal load, and $\omega = 7\frac{rad}{s}$ is the angular frequency. According to the Euler-Bernoulli beam assumptions, the peak response can be approximated as follows [38]:

$$u_{z_{max}DYN} \simeq \frac{2P_{z0}L^3}{\pi^4 EI} \frac{1}{1 - \frac{\omega}{\omega_1}} \tag{23}$$

where I is the moment of inertia of the beam cross-section. Such an approximation is valid as soon as $\omega_1 > \omega$, in which ω_1 is the bending, first fundamental angular frequency. The dynamic response was investigated using the modal superposition and the present CUF models over the time interval [0, 8] s. Table 1 shows the maximum transverse displacements at the center of the mid-space cross-section. In particular, this table compares the approximated analytical value, TE and CE models up to the third order. Figure 2 shows the

loading point transverse displacement over the time interval using the analytical solution based on Euler-Bernoulli and CE3. There is a good match between the analytical results and those from the finite element

Model	$u_{z_{max}DYN}$	ω_1
Analytical	−69.4719	14.4030
$TE3$	−70.0014	14.4006
$CE3$	−70.0019	14.3999

Table 1: Maximum transverse displacement (mm) using different theories, square beam.

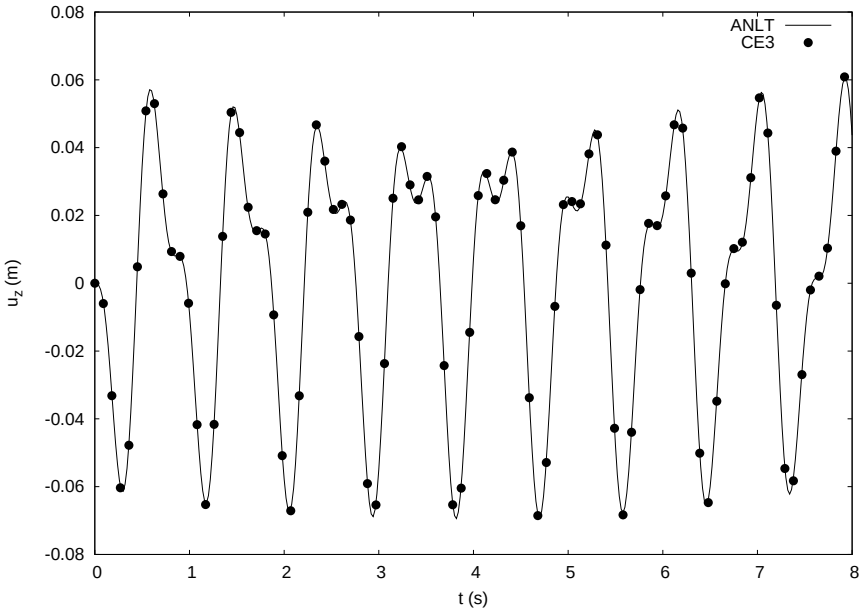

Figure 2: Transverse displacement at the center of the mid-span section for different models, square beam.

models. The use of refined models do not modify the solution to a great extent. As well known, slender, homogenous beams under bending are well modeled by classical theories. The results from CE models match perfectly the TE ones.

3.2 Sandwich Beam

This section presents the dynamic response of a clamped-clamped sandwich beam. The free vibration analysis of this beam was presented in [39]. The structure consists of two face sheets (f) bonded to a core (c). Isotropic materials were employed with E_f = 68.9 GPa, E_c = 179.014 MPa, G_f = 26.5 GPa, G_c = 68.9 MPa, ρ_f = 2687.3 kg/m^3, and ρ_c = 119.69 kg/m^3. Figure 3 shows the cross-section geometry, with h_f = 0.40624 mm, h_c = 6.3475 mm, b = 25.4 mm, and L = 1.2187 m. Two different loading cases were considered, as shown in Fig. 3. Both load cases have a sinusoidal load having amplitude F_0 = -10 N and angular frequency ω = 30 rad/s.

The time-dependent transverse displacement at the mid-span load application point are shown in Fig. 4 for various theories, whereas the maximum and minimum displacements are reported in Table 2. The maximum

deformation of the cross-section at mid-span is reported in Fig. 5 for Case 1. The results suggest that

- Overall, classical models can detect the time-dependent displacement behavior of the structures. However, significant differences were found in the maximum values due to the neglecting of torsion and the in-plane distortion of the cross-section.
- The novel CE models are as accurate as TE models and in good agreement with LE.

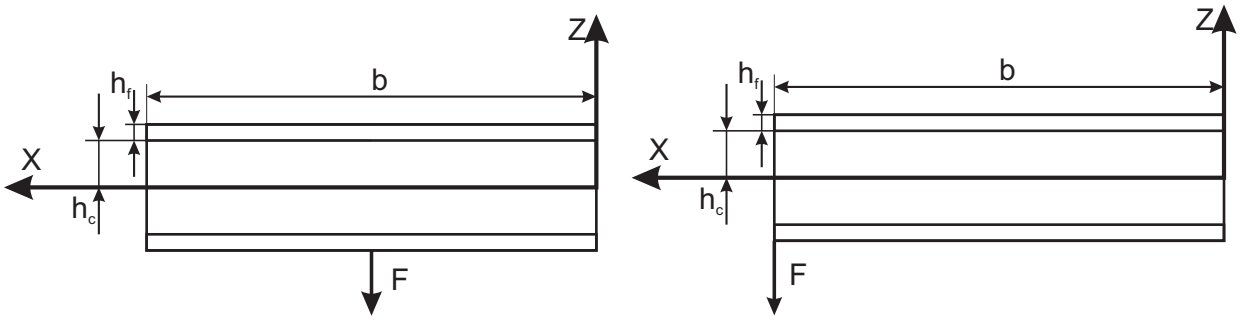

(a) Case I (b) Case II

Figure 3: Cross-section geometry of the sandwich beam and application points of the sinusoidal loads.

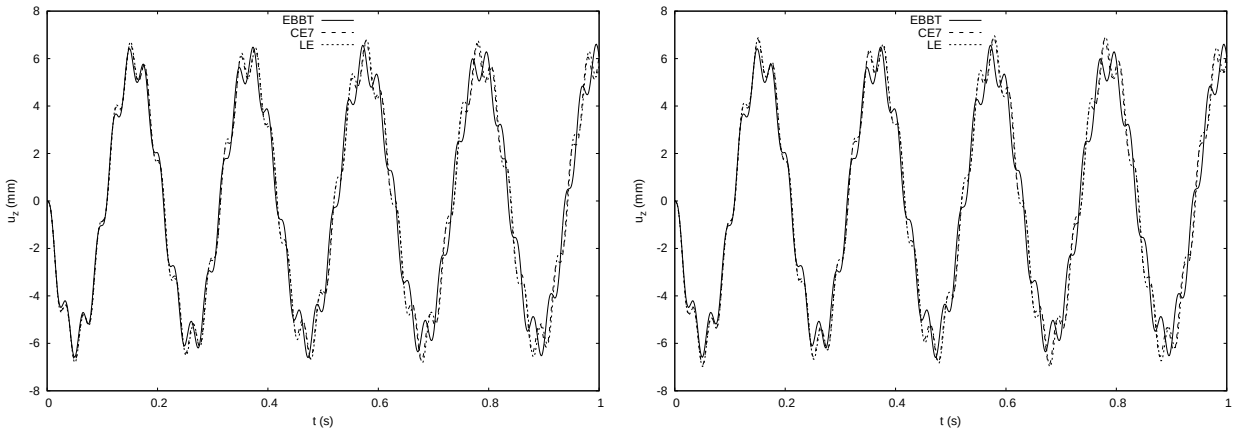

(a) Case I (b) Case II

Figure 4: Transverse displacement at the mid-span load application point for various theories, sandwich beam model.

3.3 6-layer composite box beam

A cantilever, thin walled, hollow, rectangular beam was considered. This structure has been previously investigated in [40–43] in which free vibration analyses were carried out. The structure consists of a 6-layer laminated box beam with hollow rectangular cross-section, whose dimensions are: length $L = 844.55$ mm, height $h = 13.6$ mm, width $b = 24.2$ mm and thickness $t = 0.762$ mm. Each layer has the same thickness. Two material cases were considered. The same aluminum alloy of the previous case was employed for the

Theory	DOFs	Case I		Case II	
		$u_{z_{max}}$	$u_{z_{min}}$	$u_{z_{max}}$	$u_{z_{min}}$
EBBT	93	6.612	−6.600	6.604	−6.596
TBT	155	6.612	−6.600	6.612	−6.600
$TE2$	558	6.472	−6.517	6.476	−6.521
$TE7$	3348	6.751	−6.742	6.916	−6.907
$CE2$	558	6.472	−6.517	6.476	−6.521
$CE7$	3348	6.751	−6.743	6.917	−6.908
LE	7533	6.795	−6.819	6.958	−6.982

Table 2: Maximum and minimum transverse displacement (mm) at the mid-span cross-section obtained by means of various theories, sandwich beam.

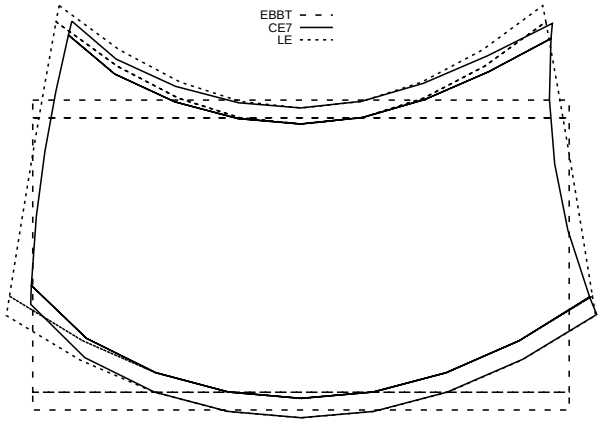

Figure 5: Deformation of the mid-span cross-section of the sandwich beam, Case 1.

isotropic case. Moreover, an orthotropic material having the following properties was considered,

$$E_1 = 141.96GPa \qquad E_2 = E_3 = 9.79GPa \quad \nu_{12} = \nu_{13} = 0.42 \quad \nu_{23} = 0.5$$
$$G_{12} = G_{13} = 6.0GPa \qquad G_{23} = 4.83GPa \qquad \rho = 1445.0\frac{kg}{m^3}$$

Different stacking sequences and ply angles were taken into account, namely the circumferentially asymmetric stiffness (CAS) and circumferentially uniform stiffness (CUS), as in Table 3. The box beam was subjected to a pressure load whose distribution across the section is shown in Fig. 6. The load was uniformly distributed in the span-wise direction while a linear distribution was considered along the width. The distributed load resultant is 10 N, whereas the height of the linear distribution is 10/L N/m. The load was modeled as a

	Flanges		Webs	
Layup	Top	Bottom	Left	Right
$CAS2$	$[30]_6$	$[30]_6$	$[30/-30]_3$	$[30/-30]_3$
$CAS3$	$[45]_6$	$[45]_6$	$[45/-45]_3$	$[45/-45]_3$
$CUS1$	$[15]_6$	$[-15]_6$	$[15]_6$	$[-15]_6$
$CUS2$	$[0/30]_3$	$[0/-30]_3$	$[0/30]_3$	$[0/-30]_3$
$CUS3$	$[0/45]_3$	$[0/-45]_3$	$[0/45]_3$	$[0/-45]_3$

Table 3: Stacking sequences of the 6-layer box beam.

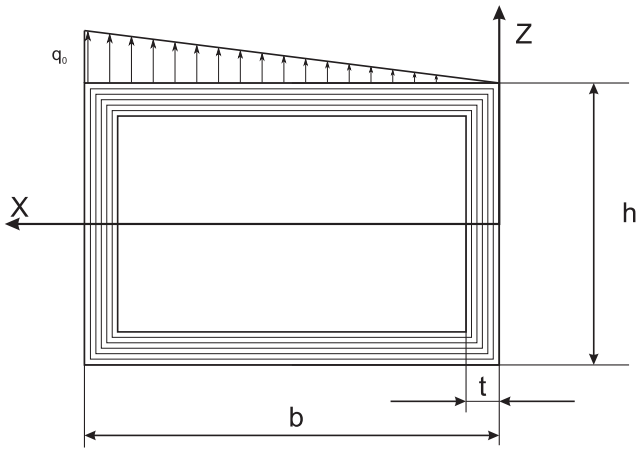

Figure 6: Load distribution for the box beam.

function of the time according to the following relation:

$$q = \begin{cases} \frac{q_0}{t_1} \cdot t, & t \in [0, t_1] \\ q_0, & t > t_1 \end{cases} \tag{24}$$

The analysis was performed considering $t_1 = 0.05$ s. Table 4 shows the transverse displacement for various models, whereas Fig. 7 shows the transverse displacement over the time interval considered. Figure 8 shows the distortion of the free tip cross-section via CE7 and LE. The results suggest that

- Perfect agreement was found between CE and TE.
- Depending on the stacking sequence, different expansion orders are needed to detect accurate results. In particular, CAS2, CAS3, and CUS1 may require seventh or higher orders while, in the other cases, third order models are enough. Similar results were found for the free vibration analysis [35].
- The distortion of the cross-section from CE models matches LE with good accuracy.

Model	$TE3$	$TE7$	$CE3$	$CE7$	LE
DOFs	930	3348	930	3348	19344
CAS2	14.085	15.000	14.087	14.992	15.247
CAS3	33.842	37.012	33.845	36.948	37.517
CUS1	8.056	8.923	8.057	8.923	9.190
CUS2	5.581	5.755	5.582	5.756	5.770
CUS3	6.529	6.590	6.529	6.591	6.560
Isotropic	3.447	3.453	3.447	3.453	3.454

Table 4: Maximum transverse displacement (mm) at the free tip of the 6-layer box beam using various models.

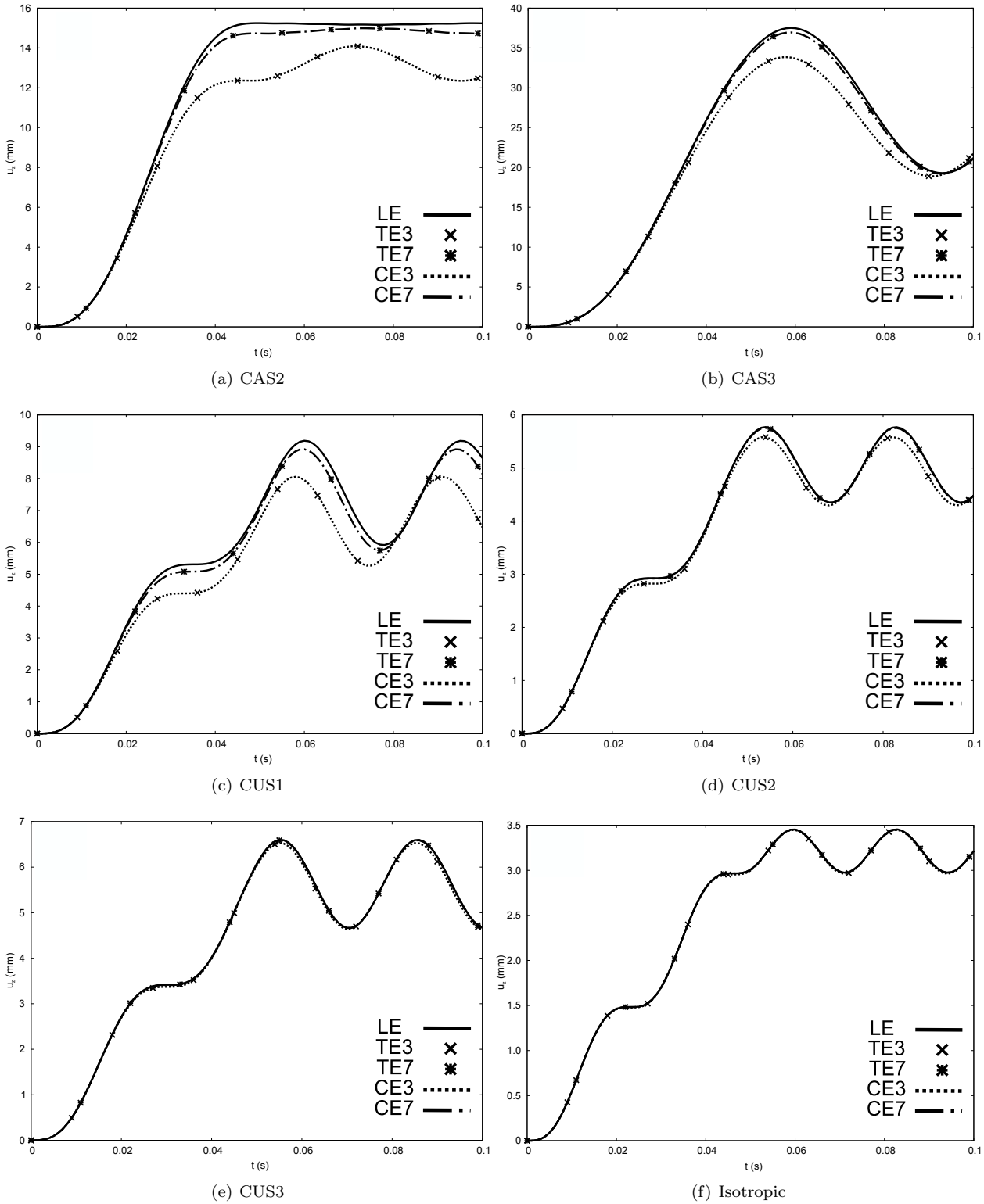

(a) CAS2 (b) CAS3

(c) CUS1 (d) CUS2

(e) CUS3 (f) Isotropic

Figure 7: Time-dependent transverse displacement at the free tip of the 6-layer box beam for various theories.

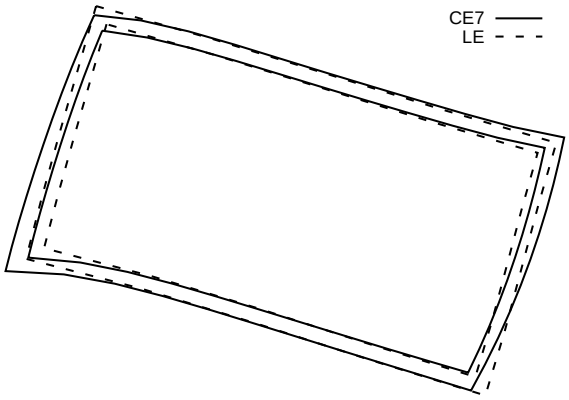

(a) CAS2, $t = 0.049$ s

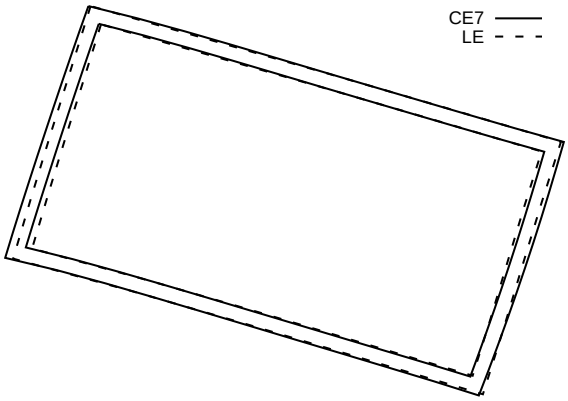

(b) CAS3, $t = 0.059$ s

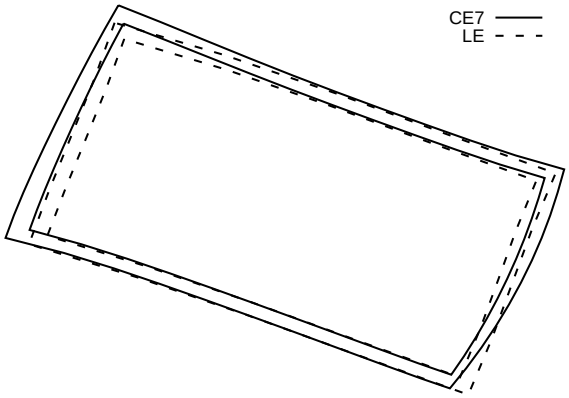

(c) CUS1, $t = 0.059$ s

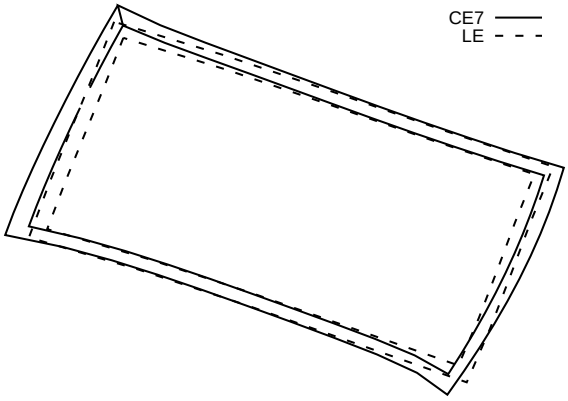

(d) CUS2, $t = 0.054$ s

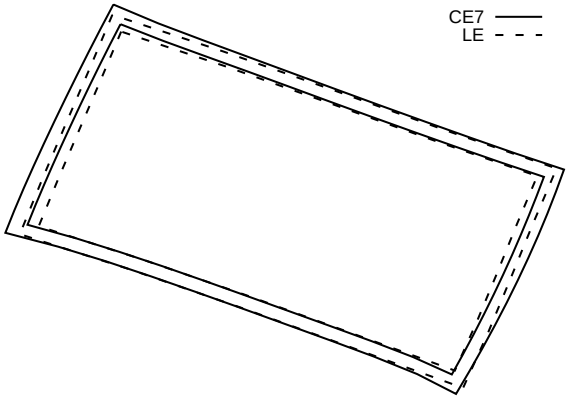

(e) CUS3, $t = 0.055$ s

Figure 8: Free tip cross-section distortion, 6-layer composite box beam.

4 Conclusions

This paper has dealt with the dynamic response of laminated and sandwich structures. 1D CUF refined structural models have been employed together with the finite element method and the mode superposition method. In particular, the Chebyshev polynomial expansions have been used to model the displacement field above the cross-section of the structure. The main aim of this paper has been the investigation of the accuracy of the Chebyshev-based 1D models for structural dynamics problems of composite structures. Numerical assessments haver dealt with compact homogeneous and sandwich beams as well as a 6-layer box structure. The results have been compared with those from Taylor and Lagrange 1D models and analytical solutions. The results suggest that

- The novel Chebyshev expansion models (CE) have proved to be as accurate as Taylor models (TE). In most cases, seventh order expansions can match the accuracy of Lagrange models (LE). However, TE and CE models usually require fewer degrees of freedom than LE.
- Higher order expansions can detect torsion, bending/torsion coupling, and cross-section distortions properly.
- As a general guideline, TE and CE should be used when global non-local effects have to be investigated. On the other hand, LE should be preferred to deal with local effects.

5 Acknowledgments

Erasmo Carrera has been partially supported by the Russian Science Foundation (Grant No. 15-19-30002).

References

[1] Euler L. *De curvis elasticis*. Geneva: Bousquet, 1744.

[2] Timoshenko S. On the corrections for shear of the differential equation for transverse vibration of prismatic bars. *Philosophical Magazine* 1922; 41: 744–746. Doi: 10.1080/14786442108636264.

[3] Timoshenko S. On the transverse vibrations of bars of uniform cross section. *Philosophical Magazine* 1922; 41: 122–131. Doi: 10.1080/14786442208633855.

[4] Kapania RK and Raciti S. Recent advances in analysis of laminated beams and plates, part ii: Vibrations and wave propagation. *AIAA Journal* 1989; 27: 935–946. URL `http://dx.doi.org/10.1007/s12046-007-0015-9`. Doi : 10.2514/3.59909.

[5] Carrera E, Pagani A, Petrolo M et al. Recent developments on refined theories for beams with applications. *Mechanical Engineering Reviews* 2015; 2(2): 14–00298–14–00298. DOI:10.1299/mer.14-00298.

[6] Timoshenko S and Goodier J. *Theory of elasticity*. New York: McGraw-Hill, 1970.

[7] Dong S, Alpdogan C and Taciroglu E. Much ado about shear correction factors in timoshenko beam theory. *International Journal of Solids and Structures* 2010; 47(13): 1651 – 1665. DOI:http://dx.doi.org/10.1016/j.ijsolstr.2010.02.018. URL `http://www.sciencedirect.com/science/article/pii/S0020768310000685`.

[8] Heyliger P and Reddy J. A higher order beam finite element for bending and vibration problems. *Journal of Sound and Vibration* 1988; 126(2): 309–326. Doi : 10.1016/0022-460X(88)90244-1.

[9] Kant T and Gupta A. A finite element model for a higher-order shear-deformable beam theory. *Journal of Sound and Vibration* 1988; 125(2): 193–202. Doi : 10.1016/0022-460X(88)90278-7.

[10] Marur S and Kant T. Free vibration analysis of fiber reinforced composite beams using higher order theories and finite element modelling. *Journal of Sound and Vibration* 1996; 194(3): 337–351. Doi : 10.1006/jsvi.1996.0362.

[11] Marur S and Kant T. On the angle ply higher order beam vibrations. *Computational Mechanics* 2007; 40(1): 25–33. Doi : 10.1007/s00466-006-0079-0.

[12] Kant T, Marur S and Rao G. Analytical solution to the dynamic analysis of laminated beams using higher order refined theory. *Composite Structures* 1997; 40(1): 1–9.

[13] Marur S and Kant T. On the performance of higher order theories for transient dynamic analysis of sandwich and composite beams. *Computers and Structures* 1997; 65(5): 741–759.

[14] Librescu L and Na S. Boundary control of free and forced oscillation of shearable thin-walled beam cantilevers. *European Journal of Mechanics, A/Solids* 1998; 17(4): 687–700.

[15] Librescu L and Na S. Dynamic response of cantilevered thin-walled beams to blast and sonic-boom loadings. *Shock and Vibration* 1998; 5(1): 23–33.

[16] Soldatos K and Elishakoff I. A transverse shear and normal deformable orthotropic beam theory. *Journal of Sound and Vibration* 1992; 155(3): 528–533. Doi : 10.1016/0022-460X(92)90717-C.

[17] Subramanian P. Dynamic analysis of laminated composite beams using higher order theories and finite elements. *Composite Structures* 2006; 73(3): 342–353. Doi : 10.1016/j.compstruct.2005.02.002.

[18] Ganesan R and Zabihollah A. Vibration analysis of tapered composite beams using a higher-order finite element. part i: Formulation. *Composite Structures* 2007; 77(3): 306–318. Doi : 10.1016/j.compstruct.2005.07.018.

[19] Orzechowski G and Shabana A. Analysis of warping deformation modes using higher order ANCF beam element. *Journal of Sound and Vibration* 2016; 363: 428 – 445. DOI:http://dx.doi.org/10.1016/j.jsv.2015.10.013. URL `http://www.sciencedirect.com/science/article/pii/S0022460X1500824X`.

[20] Carrera E. Theories and finite elements for multilayered, anisotropic, composite plates and shells. *Archives of Computational Methods in Engineering* 2002; 9(2): 87–140. Doi: 10.1007/BF02736649.

[21] Carrera E. Theories and finite elements for multilayered plates and shells: a unified compact formulation with numerical assessment and benchmarking. *Archives of Computational Methods in Engineering* 2003; 10(3): 216–296. Doi: 10.1007/BF02736224.

[22] Carrera E, Giunta G and Petrolo M. *Beam Structures Classical and Advanced Theories*. The Atrium, Southern Gate, Chichester, West Sussex, PO19 8SQ, United Kingdom: John Wiley & Sons, Ltd, 2011.

[23] Carrera E, Cinefra M, Petrolo M et al. *Finite Element Analysis of Structures through Unified Formulation*. John Wiley & Sons Ltd, 2014. ISBN 978-1-119-94121-7.

[24] Carrera E, Petrolo M and Varello A. Advanced beam formulations for free vibration analysis of conventional and joined wings. *Journal of Aerospace Engineering* 2012; 25(2). Doi: 10.1061/(ASCE)AS.1943-5525.0000130.

[25] Petrolo M, Zappino E and Carrera E. Unified higher-order formulation for the free vibration analysis of one-dimensional structures with compact and bridge-like cross-sections. *Thin Walled Structures* 2012; 56. Doi: 10.1016/j.tws.2012.03.011.

[26] Pagani A, Boscolo M, Banerjee JR et al. Exact dynamic stiffness elements based on one-dimensional higher-order theories for free vibration analysis of solid and thin-walled structures. *Journal of Sound and Vibration* 2013; 332(23): 6104–6127. Doi: 10.1016/j.jsv.2013.06.023.

[27] Dan M, Pagani A and Carrera E. Free vibration analysis of simply supported beams with solid and thin-walled cross-sections using higher-order theories based on displacement variables. *Thin-Walled Structures* 2016; 98, Part B: 478 – 495. DOI:http://dx.doi.org/10.1016/j.tws.2015.10.012. URL `http://www.sciencedirect.com/science/article/pii/S026382311530121X`.

[28] Carrera E and Varello A. Dynamic response of thin-walled structures by variable kinematic one-dimensional models. *Journal of Sound and Vibration* 2012; 331(24): 5268–5282. Doi: 10.1016/j.jsv.2012.07.006.

[29] Carrera E, Pagani A and Petrolo M. Component-wise method applied to vibration of wing structures. *Journal of Applied Mechanics* 2013; 80. Doi: 10.1115/1.4007849.

[30] Carrera E and Pagani A. Free vibration analysis of civil engineering structures by component-wise models. *Journal of Sound and Vibration* 2014; 333(19): 4597 – 4620. DOI:http://dx.doi.org/10.1016/j.jsv.2014.04.063. URL http://www.sciencedirect.com/science/article/pii/S0022460X14003708.

[31] Carrera E and Zappino E. Carrera Unified Formulation for free-vibration analysis of aircraft structures. *AIAA Journal* 2016; 54(1): 280–292.

[32] Carrera E and Pagani A. Accurate response of wing structures to free-vibration, load factors, and nonstructural masses. *AIAA Journal* 2016; 54(1): 227–241.

[33] Carrera E, Pagani A and Petrolo M. Free vibrations of damaged aircraft structures by component-wise analysis. *AIAA Journal* 2016; 54(10): 3091–3106.

[34] Carrera E, Filippi M and Zappino E. Laminated beam analysis by polynomial, trigonometric, exponential and zig-zag theories. *European Journal of Mechanics - A/Solids* 2013; 41: 58 – 69. Doi: 10.1016/j.euromechsol.2013.02.006.

[35] Filippi M, Pagani A, Petrolo M et al. Static and free vibration analysis of laminated beams by refined theory based on Chebyshev polynomials. *Composite Structures* 2015; 132: 1248 – 1259. DOI:http://dx.doi.org/10.1016/j.compstruct.2015.07.014. URL http://www.sciencedirect.com/science/article/pii/S0263822315005565.

[36] Pagani A, Petrolo M, Colonna G et al. Dynamic response of aerospace structures by means of refined beam theories. *Aerospace Science and Technology* 2015; 46: 360 – 373. DOI:http://dx.doi.org/10.1016/j.ast.2015.08.005. URL http://www.sciencedirect.com/science/article/pii/S1270963815002497.

[37] Reddy JN. *Mechanics of laminated composite plates and shells. Theory and Analysis*. 2nd ed. CRC Press, 2004.

[38] Volterra E and Zachmanoglou E. *Dynamics of Vibrations*. Ohio, USA: Charles E. Merill Books Inc., 1965.

[39] Carrera E, Filippi M and Zappino E. Free vibration analysis of laminated beam by polynomial, trigonometric, exponential and zig-zag theories. *Journal of Composite Materials* 2014; 48(19): 2299 – 2316.

[40] Armanios E and Badir A. Free vibration analysis of anisotropic thin-walled closed-section beams. *AIAA journal* 1995; 33(10): 1905–1910. Doi: 10.2514/3.12744.

[41] Gunay M and Timarci T. Free vibration of composite box-beams by Ansys. In *International Scientific Conference (UNITECH), Gabrovo, Bulgaria* 2012.

[42] Chandra R and Chopra I. Experimental-theoretical investigation of the vibration characteristics of rotating composite box beams. *Journal of Aircraft* 1992; 29(4): 657–664. Doi: 10.2514/3.46216.

[43] Carrera E, Filippi M, Mahato P et al. Advanced models for free vibration analysis of laminated beams with compact and thin-walled open/closed sections. *Journal of Composite Materials* 2015; 49(17): 2085 – 2101.